W. Nachbauer, P. Kaps, B.M. Nigg, F. Brunner, A. Lutz, G. Obkircher, and M. Mössner,
A Video Technique for Obtaining 3-D Coordinates in Alpine Skiing,
Journal of Applied Biomechanics, 1996

Reference: W. Nachbauer[1], P. Kaps[2], B.M. Nigg[3], F. Brunner[4], A. Lutz[5], G. Obkircher[6], and M. Mössner[7], *A Video Technique for Obtaining 3-D Coordinates in Alpine Skiing*, Journal of Applied Biomechanics **12** (1996), 104–115.

Abstract: A video technique to obtain 3-D data in Alpine skiing competition was investigated. The flight and landing phases of a jump were recorded during the 1994 Olympic combined downhill race. A direct linear transformation (DLT) implementation was applied, which computes the DLT parameters for each video image of each camera separately. As a consequence, one is able to pan and tilt the cameras and zoom the lenses. The problem of distributing control points in the large object space could be solved satisfactorily. The method proved to be suitable for obtaining 3-D data with reasonable accuracy, which is even sufficient for inverse dynamics. The computed resultant knee joint forces and moments compare well with results reported by other authors.

[1]Dept. of Sport Science, Univ. Innsbruck, AT. email: Werner.Nachbauer@uibk.ac.at
[2]Inst. for Basic Sciences in Engineering, Univ. Innsbruck, AT
[3]Human Performance Laboratory, Univ. Calgary, CA
[4]Dept. of Sport Science, Univ. Innsbruck, AT
[5]Dept. of Sport Science, Univ. Innsbruck, AT
[6]Dept. of Sport Science, Univ. Innsbruck, AT
[7]Dept. of Sport Science, Univ. Innsbruck, AT

1 Introduction

Film analysis of Alpine ski racing has been used for different purposes, such as performance enhancement (Fetz [5], Nachbauer [17], Förg-Rob and Nachbauer [7], Müller, Brunner, Kornexl, and Raschner [16]), safety improvement (Herzog and Read [10], Read and Herzog [20]), and studying the friction between ski and snow (Erkkilä, Hämäläinen, Pihkala, Savolainen, and Spring [4], Kaps, Nachbauer, and Mössner [11], Leino and Spring [13]). In recent years, there has been considerable progress in video technology, which is now used as an alternative to cinematography. Comparisons of film and video techniques have indicated that within a small field of view (4 m), video and film analyses provide the same accuracy (Kennedy, Wright, and Smith [12]). Angulo and Dapena [1] reported that with a large field of view (8 m), the accuracy of video analysis is inferior to that of film analysis. However, video analysis is precise enough for most practical purposes. A video technique has been proposed for conducting field research in Alpine skiing (Schaff and Hauser [21]). Fixed cameras are used, a technique that restrains the analysis to a few meters or parts of a turn.

Restricted object space due to the use of fixed cameras concerns various kinds of sport. Three-dimensional (3-D) reconstruction techniques allowing rotations of the cameras in order to follow the athlete's motion have been developed. Dapena [2] used two cameras that were free to rotate about the vertical axes. Drenk [3] and Yeadon [23] reported methods with pan and tilt cameras. Mössner, Kaps, and Nachbauer [15] introduced a direct linear transformation (DLT) method that allows the operator to pan and tilt the cameras and zoom the lenses.

The purpose of this study was to apply a video technique with pan and tilt cameras and zoom lenses in an Alpine skiing competitive environment and to test the technique's suitability for obtaining accurate 3-D data. The video technique proved to be suitable. Thus, numerous questions raised by coaches and athletes can be investigated in controlled settings as well as in competitions. The comparison of kinematic variables of skiers at different performance levels may lead to performance improvement. Kinematic analysis combined with inverse dynamics may provide insight into injury mechanisms and may bring about methods to prevent injuries. In high-speed downhill racing, anterior cruciate ligament (ACL) injuries occur frequently, predominatly during the landing phase following a jump (Figueras, Escalas, Vidal, Morgenstern, Bulo, Merino, and Espadaler-Gamisans [6]). In the present paper the method to obtain kinematic data of the jumping movement is investigated. Additionally, resultant knee joint forces and moments of one skier are presented.

2 Methods

2.1 Collection of Video Data

Video data were collected on the Russi jump during the men's special and combined downhill event of the 1994 Olympic Winter Games in Lillehammer, February 13 and 14. The flight and landing phases of all competitors, as well as the recovery phase back into the aerodynamic downhill position, were recorded. The jump, named after the former Swiss downhill racer Bernhard Russi, was located in the upper part of the downhill course at an altitude of about 800 m. The jump was caused by a natural terrain edge. Approaching the edge, the racers skied on the flat slope maintaining the tucked downhill position at a speed of more than 100 km/h. Shortly before takeoff the racers raised the low body position somewhat in order to rotate their bodies forward, thus maintaining the body orientation during flight and landing phases. The slope inclination of the landing area was about 27°. Pre-jumping was rarely used. The racers jumped between 30 to 50 m at speeds around 100 km/h.

The recording system consisted of two monochrome CCD-cameras (510 x 240 lines) and two high-speed modified Panasonic AG-1970 videocassette recorders (320 x 240 lines). The system operated on a VHS-NTSC technique basis (Motion Analysis Corporation, Santa Rosa, US-CA). The cameras were equipped with 12- to 120-mm (Angenieux, Paris, FR) and 12.5- to 75-mm (Schneider, Kreuznach, DE) zoom lenses. The lenses were zoomed in the range of 25 to 40 mm. Camera shutters were set to 1/2000 s and the f-stops between 5.6 and 11. The recordings were made on Sony S-VHS tapes. A control unit provided camera synchronization and consecutive numbering of the recorded video images. The noninterlaced video system operated at the maximum sampling frequency of 180 Hz. A power source of 110 V AC, 50-60 Hz was required.

The skiers required a distance of about 40 m for landing and recovery. In order to calibrate the large object space, 108 control points were distributed on both sides of the course (Fig 1) ensuring that in each video image 6 to 10 control points were visible. After considering safety guidelines, the jury of the competition gave us permission to establish the control point system. Two different kinds of control points were used. Black painted tennis balls (diameter = 65 mm) were attached to 250 x 200 mm white plastic plates and were screwed on poles of different lengths. The poles were placed slightly shifted along the course boundary at about 2-m intervals. In order to identify the control points in the video images, every 5th control point was a yellow tennis ball on a black plate. Additionally, on both sides close to the line of the skiers, black 100 x 200 mm carpet stripes were drilled into the snow facing the cameras. Sketches of the control points are shown in Fig 1.

Before and after the competitions, the positions of the centers of the tennis balls and the carpet stripes were determined using an SET4CII theodolite (Sokkia, JP) with a CP01 miniprism (Sokkia, JP). The tripod of the theodolite was mounted on three wooden poles that were fixed in the frozen ground. Metal fittings on the

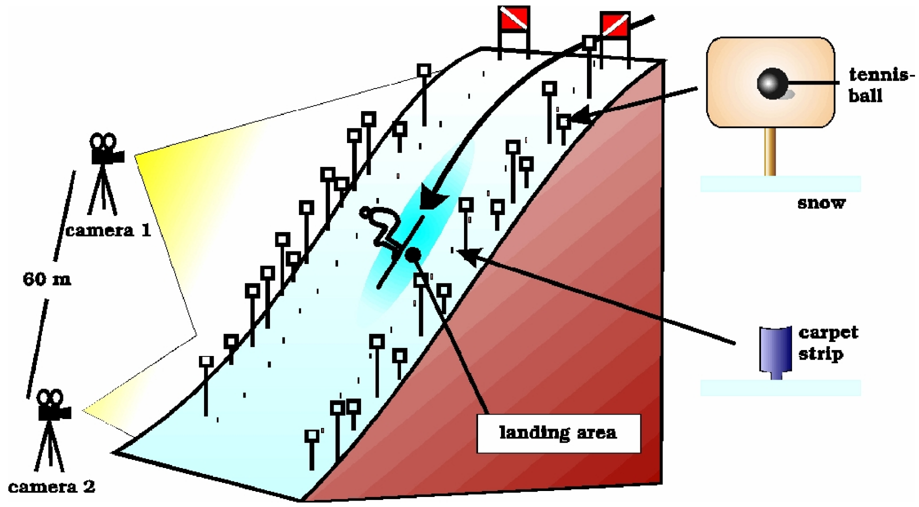

Fig. 1: Schematic illustration of the measurement site including the control points: tennis ball and carpet stripe.

wooden poles ensured the stability of the tripod. Surveying the control points took about 1.5 h. The measurements were stored on a memory card and then transferred to a notebook computer for further calculations.

In Fig 1 the camera positions are shown schematically. The cameras were panned and tilted and the lenses zoomed in order to follow the skier's motion. Camera 1 covered a field of view of approximately 8 by 6 m with an image depth of 15 m and camera 2 covered a field of view of approximately 7 by 11 m with an image depth of 30 m. The cameras were positioned to ensure angles between their optical axes between 30 and 150°. The camera operators practiced recording the competitors during the training runs.

2.2 Processing of Video Data

The videotapes were digitized using a NTSC Panasonic AG-7350 videocassette recorder and an IBM 486-compatible personal computer equipped with a 16 grey level NTSC frame grabber and a 15-in SVGA monitor. The computer was operated with the manual digitizing software of Motion Analysis Corporation (Santa Rosa, US-CA). In each video image, 8 to 10 control points, 2 points on each ski, and 19 anatomical landmarks representing the endpoints of 13 segments were digitized manually. Fig 2 shows a typical picture with the digitized points.

Our own DLT implementation was used to calculate 3-D coordinates from the digitized points (Mössner, Kaps, and Nachbauer [15]). First, the DLT parameters were computed for each video image of each camera separately and, subsequently, the 3-D coordinates of the landmarks were computed for each pair of synchronized video images. This enables the user to rotate the cameras and zoom the lenses. The method requires at least 6 control points visible in each video image. With

Fig. 2: Photograph of a video image used for digitizing.

a minimum of 6 control points, any 3 of them must not be colinear and any 4 not coplanar. For each camera, a different set of control points can be used. The main error in reconstruction arises from inaccuracies in the digitized data. The digitized data occur both in the matrix and in the right-hand side of the linear equations for calibration and reconstruction. The method of total least squares was applied (van Huffel and Vandewalle [22]). It considers errors in the matrix and the right-hand side of a system of linear equations, whereas the method of least squares would assume only errors in the right-hand side of the equations. Proper scaling of the data was essential to yield sufficiently accurate results. An orthogonal coordinate system with its origin in the average location of the control points was defined for each video image. The image coordinates were scaled in the interval of -1 to 1. The error propagation caused by solving the systems of linear equations was considerably reduced by this scaling. If the linear equations become close to singular, the scaling is absolutely necessary.

The object coordinates were presented in an orthogonal reference system with the z-axis vertical and the x- and y-axes horizontal. The traveling direction of the skier was in the x-z plane. The displacement time data were smoothed with the routine `csaps` of the MATLAB Spline Toolbox (The MathWorks Inc., Natwick, US-MA). The smoothing parameter was set to $p = 0.999$. $p = 0$ corresponds to a straight line fit and $p = 1$ to a natural cubic spline interpolant. After smoothing, the first and last 20 data points were excluded to avoid poor approximation near the interval ends. MATLAB does not provide smoothing quintic splines.

2.3 Evaluation of Measurement Errors

Errors in geodetic surveying, in reconstruction of a fixed landmark, and due to digitizing were investigated. The error was defined as absolute value of the difference between the measured value and the „true“ value. The „true“ value was the most accurate value available, for example, the arithmetic mean of two measurements in geodetic surveying or the geodetically obtained coordinate in the reconstruction of a fixed landmark. Objectivity and reliability of digitizing were examined. To determine objectivity two persons digitized the same data set. To determine reliability, the same person digitized the same data set twice. 3-D coordinates were calculated and compared with the arithmetic mean of the two digitizations, which was taken as true value. The effect of repeated digitizing was studied. The same data set was digitized three times, 3-D coordinates were calculated, averaged, and smoothed. Velocities and accelerations were computed from the smoothed average. Coordinates, velocities, and accelerations from the smoothed average were taken as true values and compared with the smoothed coordinates, velocities, and accelerations of a further digitization of the same data set. Mean errors denote the arithmetic mean of the errors taken over the values indicated in the context.

2.4 Calculation of Resultant Knee Joint Forces and Moments

Resultant knee joint forces and moments were calculated with a two-dimensional inverse dynamics approach in the sagittal plane. The skier with equipment was modeled as a linked system composed of 13 rigid segments: head, upper trunk, lower trunk and pairs of pole/hand/forearm, upper arm, thigh, shank/upper boot, and foot/lower boot/binding/ski (Fig 3). The inertial parameters of the human body segments were determined based on the geometric model of Hanavan [9] and the code of Preiss [18]. The dimensions of the geometric segments were approximated by taking 32 anthropometric measurements from the skier presented in the study. The inertial parameters of the equipment were calculated based on mass and shape measurements. Air resistance and snow friction were neglected. The influence of air resistance on knee joint resultants during the landing movement was found to be small (Read and Herzog [20]).

A one-legged landing was studied to avoid complications due to the closed loop formed by both legs in contact with the ground. The corresponding segment pairs were combined for this purpose. We used Cartesian generalized coordinates $y = (\ldots, x_i, z_i, \varphi_i, \ldots)$, where x_i, z_i denote the center of mass of segment i and φ_i denotes the orientation of this segment with respect to the vertical axis. The segments were connected by hinge joints. For a joint between the proximal end of a segment i and the distal end of a segment j, there are two kinematic constraints of the type

$$x_i + c_i \sin\varphi_i = x_j - d_j \sin\varphi_j,$$
$$z_i + c_i \cos\varphi_i = z_j - d_j \cos\varphi_j,$$

where c_i, d_j denote the distances between the joints and the centers of mass. As driving constraints the angular orientations of the segments and the coordinates of the right foot were used. The constraints can be written as an algebraic system $g(y, t) = 0$ of the same dimension as y. Thus, the equations of motion are a system

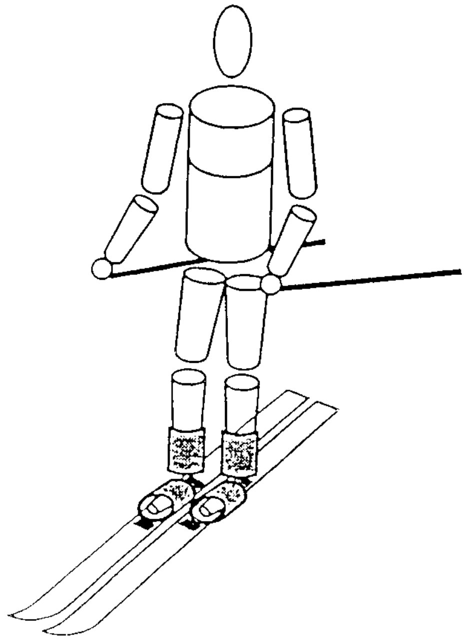

Fig. 3: Skier model with equipment.

of differential-algebraic equations:

$$M\ddot{y} = f_a + f_c, \qquad g(y,t) = 0.$$

The mass matrix $M = Diag(\ldots, m_i, m_i, I_i, \ldots)$ is diagonal, $f_a = (\ldots, 0, -m_i g, 0, \ldots)$ denotes the generalized applied forces, and f_c the generalized constraint forces. The resulting knee loads were calculated by inserting the accelerations $\ddot{y}$ obtained from the analytically differentiated smoothing splines. The computations were performed using MATLAB.

The knee joint resultants acting on the proximal end of the shank segment, that is, loads exerted by the thigh on the shank, were calculated. The resultants were expressed in a shank embedded reference frame. The y'-axis was defined by the longitudinal axis of the shank (line connecting the digitized endpoints of the shank); positive was directed proximally. The x'-axis was perpendicular to the y'-axis with positive in the anterior direction.

3 Results

3.1 Accuracy of the Measurements

The mean errors of the geodetic surveying of the 78 control points used were 0.4, 0.8, and 0.4 cm in x-, y-, and z-directions. The large errors in y-direction were mainly found at the carpet stripes. The technical accuracy of the theodolite was

Number of control points	mean error [m] x	y	z
6	0.135	0.158	0.116
7	0.075	0.108	0.070
8	0.061	0.083	0.054
9	0.059	0.079	0.050
10	0.063	0.058	0.038

Tab. 1: Mean errors in the 3-D reconstruction of a fixed landmark in 10 subsequent video frames.

5 mm + 3 mm x distance in km for distances and 1.5 mgon for angles. Thus, for an object in a distance of 0.1 km one obtains an error of $5 + 3 \cdot 0.1 = 5.3$ mm in the distance and a perpendicular deviation of $100 \cdot 0.0015 \cdot \pi/200 = 2.36$ mm.

In the reconstruction of a fixed landmark the mean errors over 10 frames were 6.3, 5.8, and 3.8 cm in the x-, y-, and z-coordinates when 10 control points were used for calibration. These errors are relatively high. The investigated landmark was located close to the edge of the jump, and in this area the angle between the optical axes of the cameras was small. Moreover, since the theodolite was positioned at the bottom of the jump, the distance to these control points was the largest resulting in the largest surveying error.

The reconstruction error was strongly affected by the number of control points used for the calibration (Tab 1). With the minimal number of 6 control points, the reconstruction error was up by a factor of 2.5. In 95 % of the images, 10 control points were used to calculate the DLT parameters. The main error in the calibration was due to the digitization of the control points. The effect of this error was averaged by using more control points than necessary. Another reason for the observed increase of accuracy with a higher number of control points may be that some of the control points were nearly colinear or coplanar. The carpet stripes were placed on the surface of the slope. Therefore, the stripes visible in a video image were approximately in the tangential plane to the surface and consequently nearly coplanar. The carpet stripes were placed in two lines on each side of the course as near as possible to the line of the skiers. Thus, three or more control points were often nearly colinear. For safety reasons, the poles with the tennis balls had to be located near the closing off the course. Although the poles differed in the height, the distance to the closing fence did not vary much. Thus, the tennis balls were also nearly coplanar. Using 6 control points with inappropriate locations for calibration could yield reconstruction errors considerably greater than 1 m. Reconstruction error is further affected by the position of the investigated landmark with respect to the calibration volume. Reconstructing landmarks about 5 m outside of the calibration volume enlarged the reconstruction error by a factor of approximately 10. No attempt was made to improve the DLT parameters by smoothing.

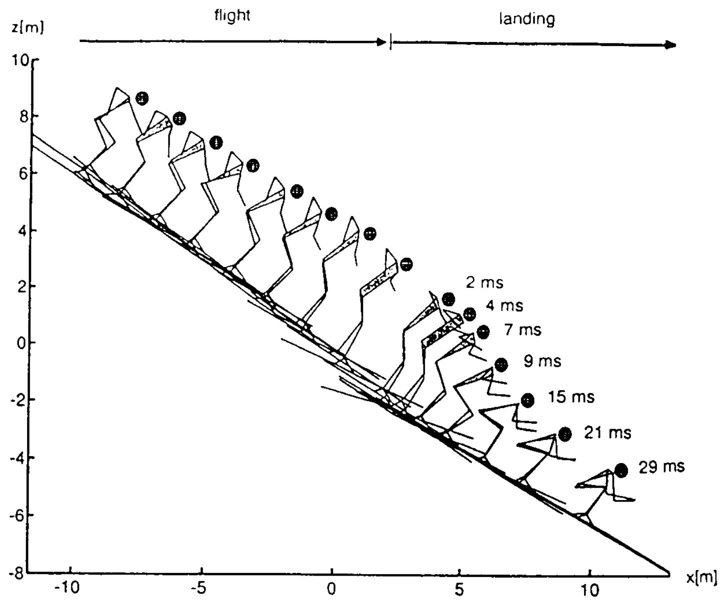

Fig. 4: Stick figure diagrams of the movement analyzed.

For objectivity, the mean errors averaged over 70 frames and 23 landmarks were 2.4, 2.3, and 1.6 cm in the x-, y-, and z-coordinates. The reliability was about 20 % better with mean errors of 1.9, 1.9, and 1.3 cm in the x-, y-, and z-coordinates. The largest errors occurred at the ski tails, which showed little contrast to the surrounding snow, and in the body landmarks of the left body side, which were frequently covered by the right body side.

Comparing the smoothed single digitization with the smoothed average of the three digitizations yielded mean errors averaged over 70 frames and 23 landmarks of 3.3, 2.4, and 2.0 cm in the x-, y-, and z-coordinates. The mean errors in the velocities were 0.20, 0.19, and 0.15 m/s and in the accelerations 3.18, 3.37, and 2.10 m/s^2 in x-, y-, and z-directions.

3.2 Resultant Knee Joint Forces and Moments

The resultant knee joint loading of one skier performing a good landing is presented next. Fig 4 shows stick figures of the analyzed skier during the last part of the flight and landing. In the landing phase a time scale is provided that corresponds to the time axis of Fig 5, in which the knee joint resultants are presented. The skier touched the ground with the left ski tail first (t = 2 ms), at t = 4 ms both skis had snow contact from the tail to the middle part, and at t = 7 ms the whole skis were on the snow (Fig 4). In this time range, the loading results might be erroneous since the coordinates of the right foot were used as a driving condition, which is not valid when the skier is in the air.

Fig 5 shows the components of the resultant knee joint force and the resultant

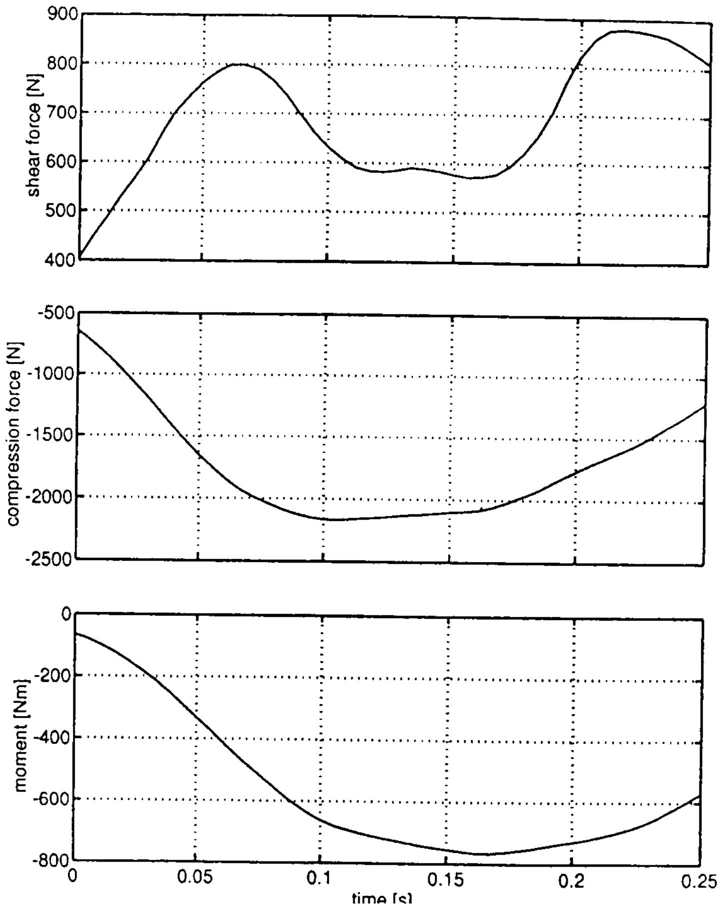

Fig. 5: a) Shear component of the resultant knee joint force acting perpendicular to the longitudinal axis of the shank. Positive forces are directed anteriorly. b) Compression component of the resultant knee joint force acting along the longitudinal axis of the shank. Negative forces are directed downward. c) Resultant knee joint moment. Extensor moments are negative and flexor moments positive.

knee joint moment as a function of time for the one-legged landing. The component acting perpendicular to the longitudinal axis of the shank was always positive varying between 400 and 880 N. This force tends to translate the shank posteriorly with respect to the thigh. The component acting along the longitudinal axis of the shank was always compressive with an extreme of -2200 N. The resulting knee joint moment was always an extensor moment with an extreme of -790 Nm.

These values compare well with results presented by other authors. Read and Herzog [20] obtained loading at the knee joint of two skiers during a World Cup Downhill race by means of inverse dynamics. Assuming a one-legged landing for the skier who executed the landing with difficulties, force extremes of 800 N in anterior and -2300 N in downward direction were calculated. Additionally, Read and Herzog consistently observed an anterior shear force and an extensor moment for the skier

Study	Shear force [N] Anterior	Posterior	Compression force [N]	Extensor moment [Nm]
Force measurements:				
Maxwell and Hull (1989)[1]	660		-625	-200
Quinn and Mote (1993)	1298	-242	-1778	-303
Inverse dynamics:				
Read and Herzog (1992)	800	-280	-2300	-630
Present study	880		-2200	-790

[1] Only averaged forces during turn were reported.

Tab. 2: Extremes of the resultant knee joint forces and moments during skiing.

who executed the landing well, which is also in agreement with our calculations. In two studies, loading at the knee joint was predicted during normal skiing (snowplow, parallel turn, Stem Cristiana turn). Maxwell and Hull [14] calculated forces and moments at the knee joints from force and moment measurements at the base of the boot neglecting inertial forces and ankle joint flexion movement. Quinn and Mote [19] improved the prediction by considering dorsiflexion at the ankle joint. The maximum of the anterior shear force was 1298 N, of the compression force -1778 N, and of the extensor moment -303 Nm (Tab 2).

4 Discussion

A DLT method to obtain 3-D data was applied in the environment of Alpine ski racing. Two main problems had to be solved before the data could be collected:

- In order to capture the skier's body as large as possible on the video image, we had to follow the skier's motion with the cameras. A DLT implementation was developed that allows the operator to pan and tilt the cameras and zoom the lenses.
- In order to calibrate the large object space where the movement took part, points with known location had to be distributed on the slope. The 108 control points used had to satisfy the geodetic requirements. A more demanding requirement was that they not disturb the athletes or cause any injury risk. Carpet stripes and poles with tennis balls were chosen as control points (Fig 1).

Errors in 3-D reconstruction are caused by errors in calibration and in the image coordinates of the landmarks. Errors in calibration are determined by the accuracy of object and image coordinates of the control points. The main reason for errors in the object coordinates of the control points used here was difficulty with identification of the centers of the control points. The centers were not marked and had to be estimated during positioning of the prism. Limitations in the technical accuracy of the theodolite and small displacements of the control points (e.g. caused by accidentally side slipping over carpet stripes during course inspection and preparation) were other error sources. Apparently moved control points were detected by resurveying. Errors in the image coordinates of the control points are discussed below. Their effect on the calibration was reduced by using 8 to 10 control points. By this and the geodetic surveying of the control points, the calibration errors could be kept so small that their influence on 3-D reconstruction was less important than the influence of errors in the image coordinates of the landmarks.

Errors in image coordinates of control points and landmarks are caused by technical limitations of the video system and by manual digitizing. Resolution of the video system was restricted by the high-speed cassette recorder, which operates in the VHS mode (320 x 240 lines). The video images covered a field of view of approximately 8 by 6 m. In the best case, each line of the video image covered a real-life distance of 800 cm / 320 = 2.5 cm in horizontal and 600 cm / 240 = 1.9 cm in vertical direction. Furthermore, the control points were often located at the margin of the images, where inaccuracies caused by lens distortion and jittering of the image were large. Control points as well as body landmarks had to be digitized manually. Digitizing body landmarks was difficult: Segment endpoints were not defined exactly, and the use of contrast markers was not possible in the competition. The landmarks on the left body side were often covered by other body parts. This was partly due to terrain restrictions regarding the camera setup. For an improvement the use of more than two cameras would be necessary. The digitizing error of body landmarks was estimated by objectivity and reliability. The mean error was smaller than 2.5 cm in each coordinate, which is surprisingly accurate.

It is interesting that the relative error in the 3-D reconstruction was in the range of laboratory measurements. Dividing a typical reconstruction error (0.03 m) by a typical length of the calibration volume (15 m) yields a relative error of 0.2 %. In laboratory measurements 0.05 to 0.5 % can be achieved. Their best accuracy can only be obtained by fixed cameras and fixed focal lengths and by averaging control point data and digitized image data.

As discussed previously, the raw data are erroneous. For various investigations the computation of accelerations and forces is of interest. By interpolation we obtained irregularly oscillating accelerations in the order of magnitude of 10^4 m/s^2. Therefore, smoothing was a necessity. As well known, there are a variety of different smoothing techniques, all of which provide better results with a higher number of data points. The sampling rate of 180 Hz provided enough data points for smoothing. The mean absolute difference between raw and smoothed data was less than 3 cm (in x- and z-directions) for the chosen smoothing parameter. Since this difference is small, there was no oversmoothing. One could suspect undersmoothing, but this would lead to strong oscillations in accelerations, which was not the case.

Our objective in measuring phases of the Russi jump was to improve understanding of ACL injury mechanisms occurring during landing in downhill skiing.

Further analyses will include determining of knee joint resultants of several racers performing the landing movement differently and estimating of the forces in the ACL. Being aware of the limitations of the inverse dynamics approach, we developed a simulation model (Gerritsen, Nachbauer, and Bogert [8]). The video data were used as initial values for the simulations and for validation of the model. The validated simulation model will be used to study the influence of isolated variables by varying them systematically.

Acknowledgments

The study was supported by the IOC Medical Commission, the International Ski Federation, and the Austrian Ski Federation. We are grateful to Thomas Weinold for instructions in geodetic surveying and Thomas Fetz for performing the MATLAB computations.

References

[1] R.M. Angulo and J. Dapena, *Comparison of Film and Video Techniques for Estimating Three-Dimensional Coordinates within a Large Field*, International Journal of Sport Biomechanics **8** (1992), 145–151.

[2] J. Dapena, *Three-Dimensional Cinematography with Horizontal Panning Cameras*, Sciences et Motricité **1** (1978), 3–15.

[3] V. Drenk, *Erarbeitung von photogrammetrischen Auswerteverfahren für den Einsatz schwenkbarer Kameras in der Leistungssportforschung (Photogrammetric Analysis Methods for Pan and Tilt Cameras in Sports Research)*, Ph.D. Thesis, Forschungsinstitut für Körperkultur und Sport, Leipzig, DE, 1988.

[4] J. Erkkilä, T. Hämäläinen, P. Pihkala, S. Savolainen, and E. Spring, *A Cinematographic Method for Determination of the Kinetic Friction of Skis on Snow*, Report Series in Geophysics, vol. 21, University of Helsinki, FI, 1985.

[5] F. Fetz, *Biomechanische Analyse alpiner Zieleinfahrtechniken (Biomechanical analysis of finishing techniques in alpine ski racing)*, Zur Biomechanik des Schilaufs (F. Fetz, ed.), Inn-Verlag, Innsbruck, AT, 1977, 68–79.

[6] J.M. Figueras, F. Escalas, A. Vidal, R. Morgenstern, J.M. Buló, J.A. Merino, and J.M. Espada-Gamisans, *The Anterior Cruciate Ligament Injury in Skiers*, Skiing Trauma and Safety 6th vol., ASTM STP 938 (Philadelphia, US-PA) (C.D. Mote and R.J. Johnson, eds.), American Society for Testing and Materials (ASTM), 1987, pp. 55–60.

[7] W. Förg-Rob and W. Nachbauer, *Use of Spline-Functions in the Smoothing of Film Data for Slalom Ski Racers*, International Journal of Sport Biomechanics **4** (1988), 166–177.

[8] K.G.M. Gerritsen, W. Nachbauer, and A.J. van den Bogert, *Simulation of Landing Movement in Downhill Skiing: Validation Using Experimental Data*, Proceedings of the Eighth Biennial Conference (Calgary, CA), Canadian Society for Biomechanics, 1994, pp. 192–163.

[9] E.P. Hanavan, *A Mathematical Model of the Human Body*, AMRL-TR-64-102, Wright-Patterson Air Force Base, US-OH, 1964.

[10] W. Herzog and L. Read, *Anterior Cruciate Ligament Forces in Alpine Skiing*, Journal of Applied Biomechanics **9** (1993), 260–278.

[11] P. Kaps, W. Nachbauer, and M. Mössner, *Determination of Kinetic Friction and Drag Area in Alpine Skiing*, Ski Trauma and Skiing Safety: 10th Volume, ASTM STP 1266 (Philadelphia, US-PA) (C.D. Mote, R.J. Johnson, W. Hauser, and P.S. Schaff, eds.), American Society for Testing and Materials (ASTM), 1996, pp. 165–177.

[12] P.W. Kennedy, D.L. Wright, and G.A. Smith, *Comparison of Film and Video Techniques for Three-Dimensional DLT Repredictions*, International Journal of Sport Biomechanics **5** (1989), 457–460.

[13] M.A.H. Leino and E. Spring, *Determination of the Coefficient of Kinetic Friction between Ski and Snow from Gliding Velocity of a Skier*, Report Series in Geophysics, vol. 19, University of Helsinki, FI, 1984.

[14] S.M. Maxwell and M.L. Hull, *Measurement of Strength and Loading Variables on the Knee During Alpine Skiing*, Skiing Trauma and Safety, 7th vol., ASTM STP 1022 (Philadelphia, US-PA) (R.J. Johnson and C.D. Mote, eds.), American Society for Testing and Materials (ASTM), 1989, pp. 231–251.

[15] M. Mössner, P. Kaps, and W. Nachbauer, *A Method for Obtaining 3-D Data in Alpine Skiing Using Pan and Tilt Cameras with Zoom Lenses*, Skiing Trauma and Safety, 10th vol., ASTM STP 1266 (Philadelphia, US-PA) (C.D. Mote, R.J. Johnson, W. Hauser, and P.S. Schaff, eds.), American Society for Testing and Materials (ASTM), 1996, pp. 155–164.

[16] E. Müller, F. Brunner, E. Kornexl, and C. Raschner, *Biomechanische Analyse von Starttechniken im alpinen Skirennlauf (Biomechanical Analysis of Starting Techniques in Alpine Ski Racing)*, Biomechanik der Sportarten. Band 2: Biomechanik des alpinen Skilaufs (F. Fetz and E. Müller, eds.), Ferdinand Enke Verlag, Stuttgart, DE, 1991, pp. 112–123.

[17] W. Nachbauer, *Fahrlinie in Torlauf und Riesentorlauf (Line in Slalom and Giant Slalom)*, Leistungssport **17** (1987), 17–21.

[18] R. Preiss, *PHANA, Fortran Program to Compute the Inertia Parameter according to Hanavan*, Tech. Report, Department of Sport Science, University of Frankfurt, DE, 1983.

[19] T.P. Quinn and C.D. Mote, *Prediction of the Loading Along the Leg During Snow Skiing*, Skiing Trauma and Safety, 9th vol., ASTM STP 1182 (Philadelphia, US-PA) (R.J. Johnson, C.D. Mote, and J. Zelcer, eds.), American Society for Testing and Materials (ASTM), 1993, pp. 128–149.

[20] L. Read and W. Herzog, *External Loading at the Knee Joint for Landing Movements in Alpine Skiing*, International Journal of Sport Biomechanics **8** (1992), 63–80.

[21] P.S. Schaff and W. Hauser, *3-D Video Motion Analysis on the Slope - A Practical Way to Analyze Motion Patterns in Alpine Skiing*, Skiing Trauma and Safety, 9th vol., ASTM STP 1182 (Philadelphia, US-PA) (R.J. Johnson, C.D. Mote, and J. Zelcer, eds.), American Society for Testing and Materials (ASTM), 1993, pp. 165–177.

[22] S. van Huffel and J. Vandewalle, *The Total Least Squares Problem. Computational Aspects and Analysis*, Society for Industrial and Applied Mathematics (SIAM), Philadelphia, US-PA, 1991.

[23] M.R. Yeadon, *A Method for Obtaining Three-Dimensional Data on Ski Jumping Using Pan and Tilt Cameras*, International Journal of Sport Biomechanics **5** (1989), 238–247.